The 2015 World Congress on
Advances in Structural Engineering and Mechanics (ASEM15)
Incheon, Korea, August 25-29, 2015

Structural behavior of yielding shear expanded metal panels

C. Graciano[1)], P. Teixeira[2)], G. Martínez[3)]

[1)] *Universidad Nacional de Colombia, Facultad de Minas, Departamento de Ingeniería Civil, Medellín, Colombia*
[2), 3)] *Universidad Simón Bolívar, Departamento de Mecánica, Apdo. 89000, Caracas 1080-A, Venezuela*
[1)] *cagracianog@unal.edu.co*

ABSTRACT

This paper aims at investigating the quasi-static response of yielding shear expanded metal panels. The study is conducted by means of nonlinear finite element analysis of the expanded metal panel embedded in a pinned rigid frame similar to the typical experimental mounting of shear tests. The model was validated against experimental results available in the literature. Thereafter, the numerical model is used to study the structural behavior of the panels in depth. A parametric analysis is conducted to investigate the influence of cell geometry parameters by analyzing three different cell types at different orientations, the effect of the panel size on the shear response of the panel. The results show that shear response depends mainly of cell geometry and panel length while panel height effect is almost negligible. Finally, expanded metal panels subjected to shear loading exhibited a local stable collapse mechanism.

1. Introduction

In current structural engineering practice, steel plate shear walls are built-up members composed of a robust frame and weak infill plates. Their resistance depends on tension field action in the infill in order to provide lateral load strength to the frame. Therefore, it is necessary to address appropriately the strength of infill plates to avoid the introduction of excessive force that may increase column demand in the framing members (Bhowmick 2009). In the literature, there are different ways to reduce this force, by either weakening the infill plate through perforations (Vian 2005, Bhowmick, 2014, Bhowmick et al. 2014) or slits (Egorova et al. 2014, Hitaka and Matsui 2003, Cortes and Liu 2011), using low yield carbon steel (Vian and Bruneau 2005) or using very thin plates (Vian and Bruneau 2005, Berman and Bruneau 2005).

Recent investigations conducted by Bhowmick (2014) have demonstrated that there is a reduction in shear strength for steel plate shear walls with a single perforation as the diameter of the hole increases. Bhowmick et al. (2014) conducted a nonlinear analysis on the influence of circular perforations on the shear strength of shear walls. The results showed that both, the diameter of the holes and their spacing control the

decrease in shear strength of the system. Expanded metal panels exhibit various advantages for shear wall systems. These panels are manufactured in a single process upon in-line expansion of partially slit metal sheets, producing diamond like patterns, leading to a lightweight mesh composed of strands connected in a continuous manner through nodes. In addition, these meshes are usually made from low yield carbon steel. Expanded metal panels are basically produced in two basic types: Standard (EMS) and Flattened (EMF) (EMMA 2012).

Smith et al. (Smith et al. 2009) conducted a review of international patents regarding possible applications of expanded metal meshes covering several areas within the fields of structural engineering, crashworthiness and biomechanics. It has been demonstrated that expanded metal meshes can absorb energy by plastic deformation mechanisms (Graciano et al. 2009, Graciano et al. 2012, Martínez et al. 2013, Smith et al. 2014, Smith et al. 2014). Dung and Plumier (2010), Dung (2011) conducted an investigation aimed at finding an application for expanded metal meshes for seismically retrofitting of reinforced concrete moment resisting frames. A complete study was conducted on pure shear behavior of expanded metal meshes subjected to monotonic and quasi-static cyclic loading, using experimental, theoretical and numerical approaches.

This paper is aimed at studying the structural behavior of expanded metal panels subjected to shear loading. Firstly, the study is conducted by means nonlinear finite element analysis of EMS panels. Once the numerical models are validated with experimental results taken from the literature, a parametric analysis is conducted to investigate the influence on the shear response of: a) the cell orientation; b) the size of the expanded metal cell, including the strand cross section; and finally c) the material properties. The results shows the suitability of expanded metal panel for steel plate shear walls.

2. Numerical model

This section presents a numerical study on the nonlinear shear response of EMS panels. A series of finite element models are developed using the implicit static structural solver ANSYS (2009). Large deflections are considered into the model to capture the nonlinear response of the shear panel due to metal plasticity, out-of-plane plate buckling and high strain levels.

Fig. 1 shows a schematic view of the shear tests, as conducted experimentally in Dung (2011). A hinged frame is used to load the infill panels (EMS); the frame is significantly stiffer than the infill. The assembly is clamped at the base, and laterally loaded in the upper part of the frame. Hence, a pure shear state is guaranteed at the inner panel, and the strain compatibility at the connection between the panel and the frame has not significant influence in the response as demonstrated by Dung (2011).

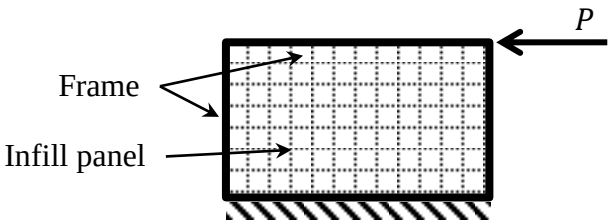

Fig. 1. Schematic view of the pushover test.

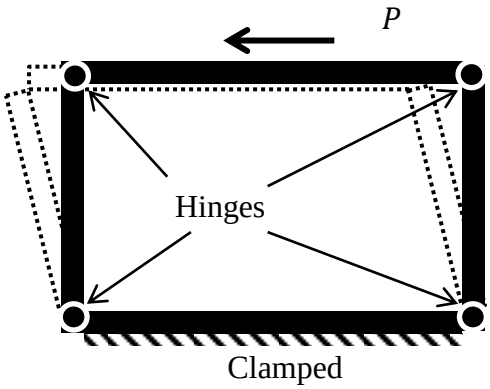

Fig. 2. Frame boundary conditions.

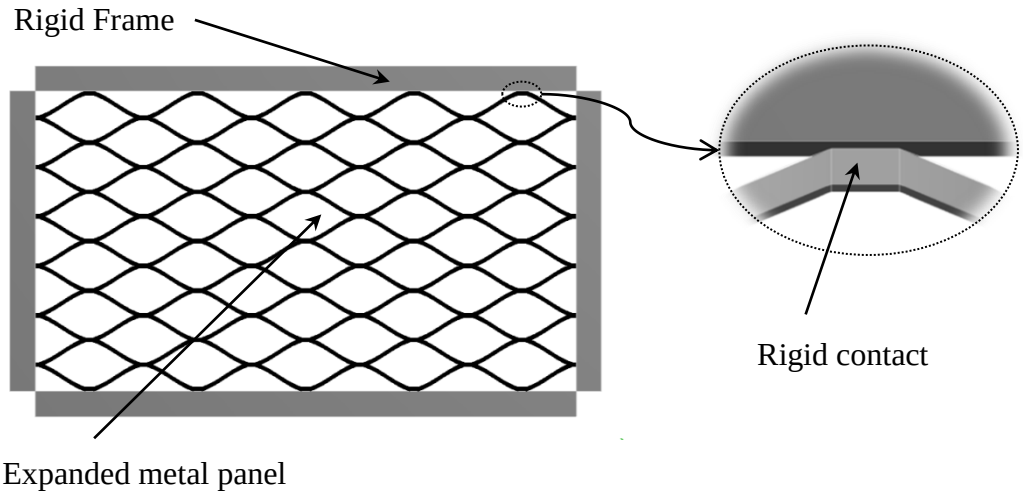

Fig. 3. Schematic view of the shear test assembly.

Accordingly, in order to apply the pure shear condition in the computational model, a rigid frame composed of four pin-connected rigid bars was used to achieve a desired drift as shown in Fig. 2, similar to the experimental mounting carried out in Dung (2011), which is used to model a building frame.

Summing up, the model has the following advantages:

- The frame is significantly rigid ensuring a pure shear condition at the infill panel,
- It is easier to handle since no mesh is needed to discretize the frame geometry and the connection between the frame and the panel is modeled as a rigid contact, reducing computational costs.

- It has also zero stiffness to shear deformation, meaning that the mechanical response of the infill is not affected by the frame, and the measured load capacity is only attributed to the panel stiffness.

The boundary conditions shown in Fig. 2 replicate those used in Dung (2011) where a tangential load P is applied to the hinged frame. In addition, the shear load P is displacement controlled to achieve a better convergence in the nonlinear numerical solution. A more detailed description of the assembly is presented in Fig. 3.

An individual cell geometry is schematized in Fig. 4, where L_1 is the cell length, L_2 is the cell height, t the strand thickness, and w the strand width. An additional parameter to be considered is the cell orientation, that can be oriented horizontally $\alpha = 0°$, and vertically $\alpha = 90°$ as shown in Fig. 5.

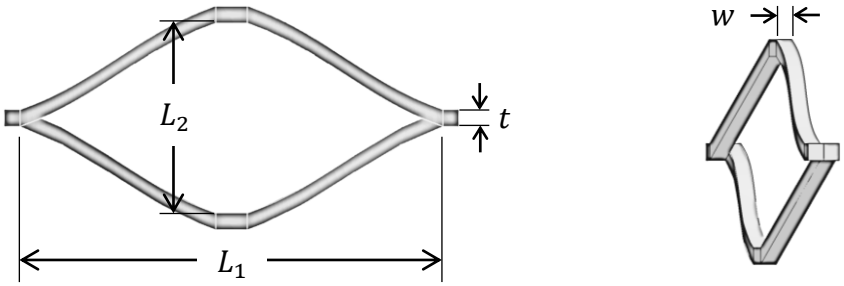

Fig. 4. Nomenclature for an expanded metal cell.

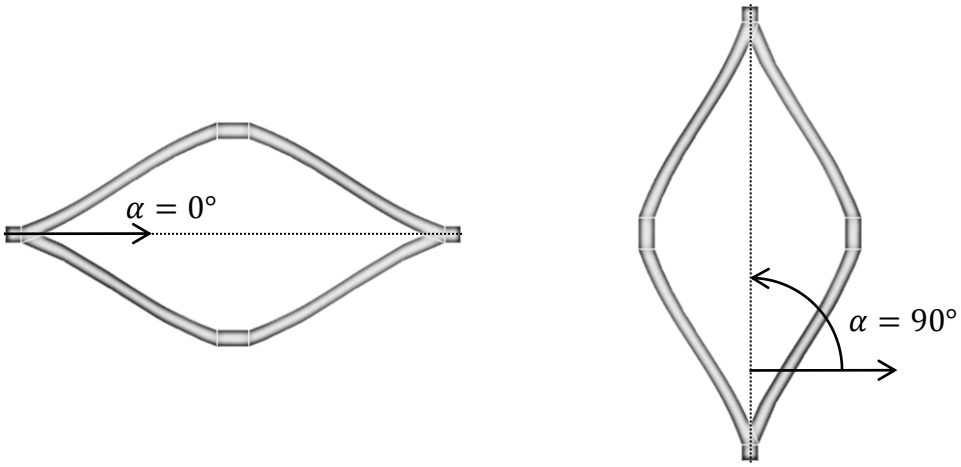

Fig. 5. Cell orientations.

The expanded metal cells in the panels were modeled with hexahedral high order SOLID 186 elements (ANSYS 2009) suitable for large strain analyses. Fig. 6 shows an outline of the mesh configuration for the two cell geometries. The material was modeled using a classical bilinear isotropic hardening model (strain rate independent) that uses two slopes (elastic and plastic) to represent the stress-strain behavior of the material.

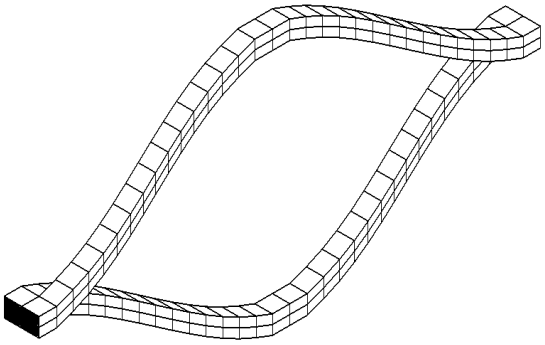

(a) EMS cell
Fig. 6. Finite element meshe.

Shear tests were conducted through a quasi-static analysis. A load-step control strategy to solve the nonlinear problem is adopted. Initially, the load is divided into 50 steps, and the convergence rate of the Newton–Raphson scheme adjusts the load increment step to optimize time solution in order to achieve convergence and the final solution.

3. Validation.

For validation purposes, four numerical models were elaborated, for each orientation two models, one with EMF and one with EMS panels. Subsequently, a set of shear tests were performed using the same dimensions of the experimentally tested EM panels carried out by [18]. Correspondingly, Fig. 7 shows the panel dimensions $h = 695mm$ and $L_p = 1095mm$, meaning $N_c = 12$ and $N_r = 15$. The cell geometry corresponds to Type A as given in Table 1.

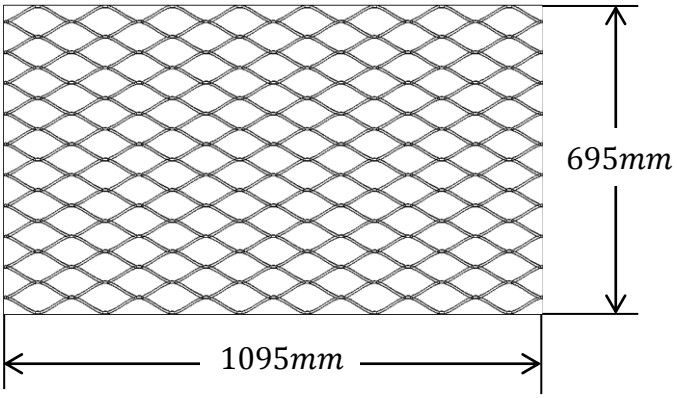

Fig. 7. Validation panel dimensions

Regarding material properties, the corresponding yield strength for EMS panels is $S_y = 337MPa$; this value was obtained experimentally by Dung (2011). Further information regarding material specifications was not available.

Table 1 Expanded metal cell dimensions.

Type	L_1 (mm)	L_2 (mm)	w (mm)	t (mm)
A	80	36	3.2	3
B	58	28	5.2	5
C	85	20.6	7.65	6.35

Then, the finite element models were validated by comparison between the numerical results with the experimental measurements obtained in [18]. Fig. 8 shows the load-drift response of the tested EM panels.

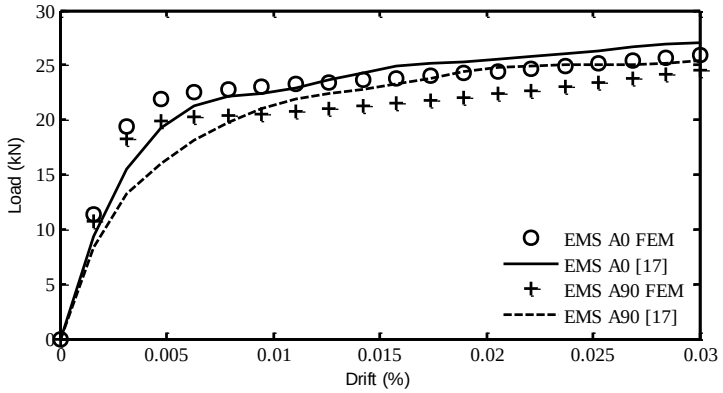

Fig. 8. Comparison between experimental and numerical results for EMS panels.

In Fig. 8, a very good agreement is achieved when comparing the load-drift responses obtained numerically and experimentally for EMS panels at both 0° and 90°. Though, it is observed that the panels with 0º configuration can sustain slightly more load than 90º panels. It happens since the shear load is aligned with the main diagonal of the expanded metal cell, this finding is similar to that obtained in previous works on EMS tubes subjected to crushing loads.

4. Parametric analysis

In this section, a parametric analysis is conducted to study the effect of cell dimensions for the three expanded metal geometries given in Table 1. The panel size is given by the amount of cell rows and columns, since the infill panel is composed by an exact amount of cells. Three types of meshes are used in the study, namely Type A, Type B and Type C. For each EM type cell, different panel sizes are simulated according to the dimensions reported in Table 2. A total of 54 models were analyzed.

The behavior of an expanded metal panel under shear loading depends on frame size, cell geometry and material properties. Frame size parameters are depicted in Fig. 9, where h is the panel height, which is proportional to the number of panel cell rows. The panel length L_p is proportional to the number of panel cell columns, hence L_p and

h can be calculated using Eqs. (1) and (2), respectively. Since the internal cell dimensions are given, a small portion of strands should be added in order to obtain the complete panel size.

$$L_p = N_c\,(L_1 + 2w) \tag{1}$$
$$h = N_r\,(L_2 + 2t) + t \tag{2}$$

The panel drift d can be calculated using Eq. (3).

$$d = u/h \tag{3}$$

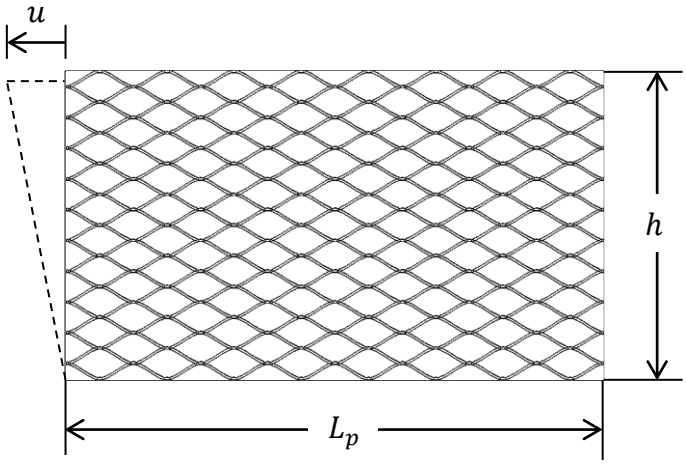

Fig. 9. Panel dimensions

In Tables 2 and 3, the number of cells in the transversal direction (columns) N_c was varied from 8 to 16, and in the vertical direction, the number of cells (rows) was varied from 10 to 28. The material properties in the parametric analysis for EMS geometries were considered as follows, the material used was an ASTM 579 as reported in [20], with a yield strength S_y=250 MPa, Young's modulus E=205 GPa, and tangent modulus E_t=2100 MPa as shown in Fig. 10.

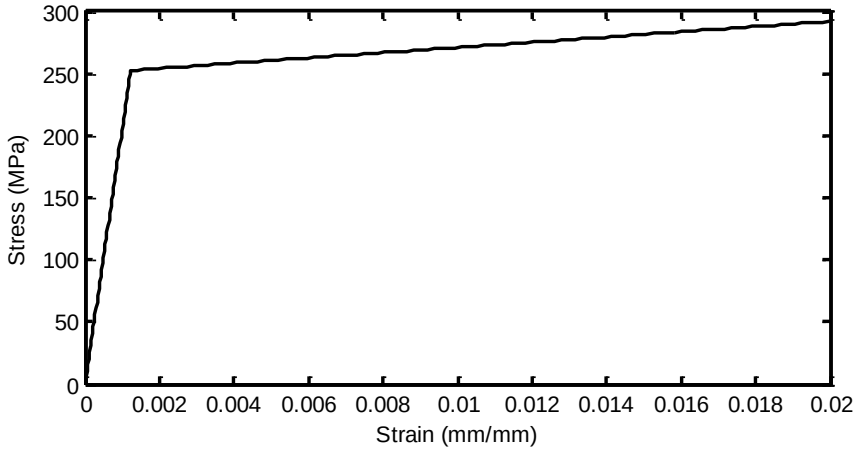

Fig. 10. Stress-strain curve of expanded metal steel [20].

All simulations were carried to obtain the load drift response of each expanded metal up to a drift value of $d = 0.1$. Although seismic excitations and maximum allowable drift in buildings are less than 3%.

From the drift response the initial stiffness K_0, the yielding load P_y, the post-yielding stiffness K_p, and the yielding load per unit panel length P_L are measured to analyze in detail the shear response of each panel. Fig. 11 shows a typical nonlinear curve describing the nomenclature used herein. The initial stiffness is measured using a linear fit to the first points of the load-drift curve, while the post-yielding stiffness is measured using another linear fit to the post-yielding points of the curve. The yielding load P_y is measured as the load that makes an equivalent permanent drift deformation $d = 0.002$, and P_L can be calculated by Eq. (4).

$$P_L = P_y / L_p \tag{4}$$

Table 2. Geometry and dimensions of EMS panels.

Panel	N_c	N_r	L_p(mm)	h (mm)	*Panel*	N_c	N_r	L_p(mm)	h (mm)
EMS A0 8x10	8	10	688	395.2	EMS A90 16x4	16	4	681.6	344
EMS A0 8x12	8	12	688	473.6	EMS A90 16x6	16	6	681.6	516
EMS A0 8x14	8	14	688	552	EMS A90 16x8	16	8	681.6	688
EMS A0 12x15	12	15	1032	591.2	EMS A90 24x6	24	6	1020.8	516
EMS A0 12x18	12	18	1032	708.8	EMS A90 24x9	24	9	1020.8	774
EMS A0 12x21	12	21	1032	826.4	EMS A90 24x12	24	12	1020.8	1032
EMS A0 16x20	16	20	1376	787.2	EMS A90 32x8	32	8	1360.0	688
EMS A0 16x24	16	24	1376	944	EMS A90 32x12	32	12	1360.0	1032
EMS A0 16x28	16	28	1376	1100.8	EMS A90 32x16	32	16	1360.0	1376
EMS B0 8x10	8	10	547.2	335	EMS B90 16x4	16	4	608	273.6
EMS B0 8x12	8	12	547.2	401	EMS B90 16x6	16	6	608	410.4
EMS B0 8x14	8	14	547.2	467	EMS B90 16x8	16	8	608	547.2
EMS B0 12x15	12	15	820.8	500	EMS B90 24x6	24	6	912	410.4
EMS B0 12x18	12	18	820.8	599	EMS B90 24x9	24	9	912	615.6
EMS B0 12x21	12	21	820.8	698	EMS B90 24x12	24	12	912	820.8
EMS B0 16x20	16	20	1094.4	665	EMS B90 32x8	32	8	1216	547.2
EMS B0 16x24	16	24	1094.4	797	EMS B90 32x12	32	12	1216	820.8
EMS B0 16x28	16	28	1094.4	929	EMS B90 32x16	32	16	1216	1094.4
EMS C0 8x10	8	10	802.4	275.85	EMS C90 20x4	20	4	666.0	401.2
EMS C0 8x12	8	12	802.4	329.75	EMS C90 20x5	20	5	666.0	501.5
EMS C0 8x14	8	14	802.4	383.65	EMS C90 20x6	20	6	666.0	601.8
EMS C0 12x15	12	15	1203.6	410.6	EMS C90 30x4	30	4	999.0	401.2
EMS C0 12x18	12	18	1203.6	491.45	EMS C90 30x6	30	6	999.0	601.8
EMS C0 12x21	12	21	1203.6	572.3	EMS C90 30x8	30	8	999.0	802.4
EMS C0 16x20	16	20	1604.8	545.35	EMS C90 40x6	40	6	1332.0	601.8
EMS C0 16x24	16	24	1604.8	653.15	EMS C90 40x8	40	8	1332.0	802.4
EMS C0 16x28	16	28	1604.8	760.95	EMS C90 40x10	40	10	1332.0	1003.0

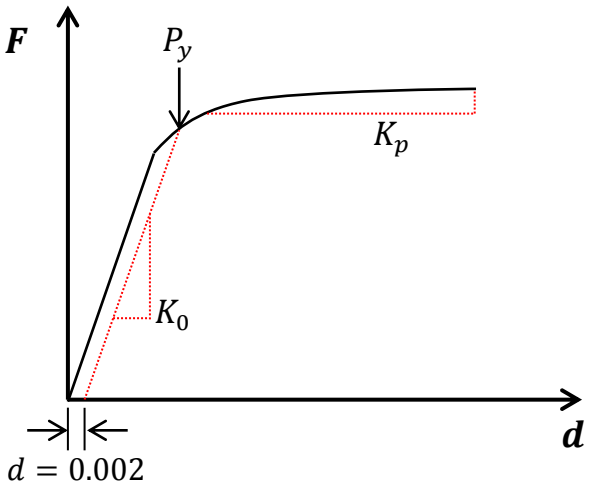

Fig. 11. Load-drift response nomenclature

4.1 Shear response for EMS panels

Figs. 12 and 13 show the load-drift responses obtained from the numerical simulations for EMS panels with α=0° and α=90°. These figures show the effect of the panel length (L_p) and height (h) on the shear response for the EMS panels described in Table 2. The shear behavior can be divided into two stages, a linear elastic until the yield drift is reached, thereafter the slope in the load-drift response is reduced significantly to the post-yield stiffness K_p.

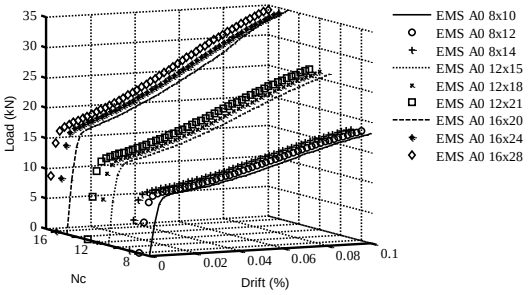

(a) Type A

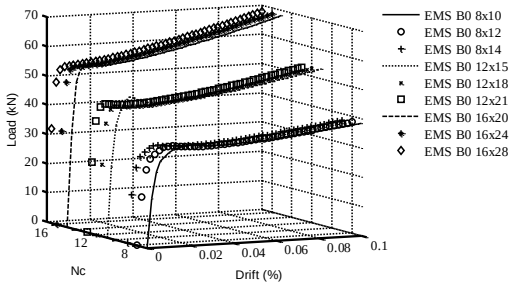

(b) Type B

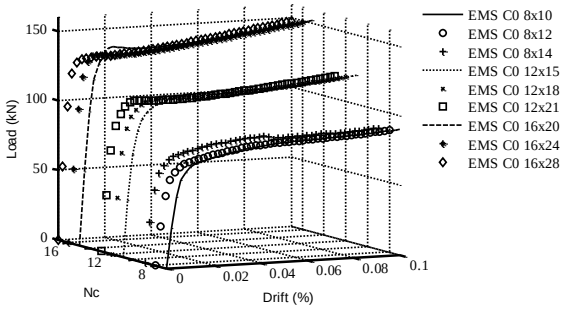

(c) Type C

Fig. 12. Load-drift responses for EMS panels with α=0°.

Fig. 12a shows the load-drift responses for EMS panels Type A with α=0º (EMS A0). The response begins with a linear behavior followed by a smooth transition toward a plastic behavior after the yielding load P_y is achieved. All panels experiments a response with a similar shape, but a linear increase in the load amplitude is found when increasing the number of columns, this means that the panel shear strength increases with the panel length, *i.e.* for a fixed number of columns or panel length, the number of panel rows or height has no effect on the response. It is worth noticing that changing panel height affects the lateral displacement of the frame, but the drift is independent of this dimension which remains fixed to a limit value $d = 0.1$.

Load-drift responses for panels EMS B0 and EMS C0 are shown in Figs. 12b and 12c, respectively. Their structural behavior is similar to the one observed for panels EMS A0. However, significant differences in load magnitude are retrieved due to an increase in the size of the EMS cells. Type C panels have the largest strand cross section (see Table 1); hence these achieve higher strengths.

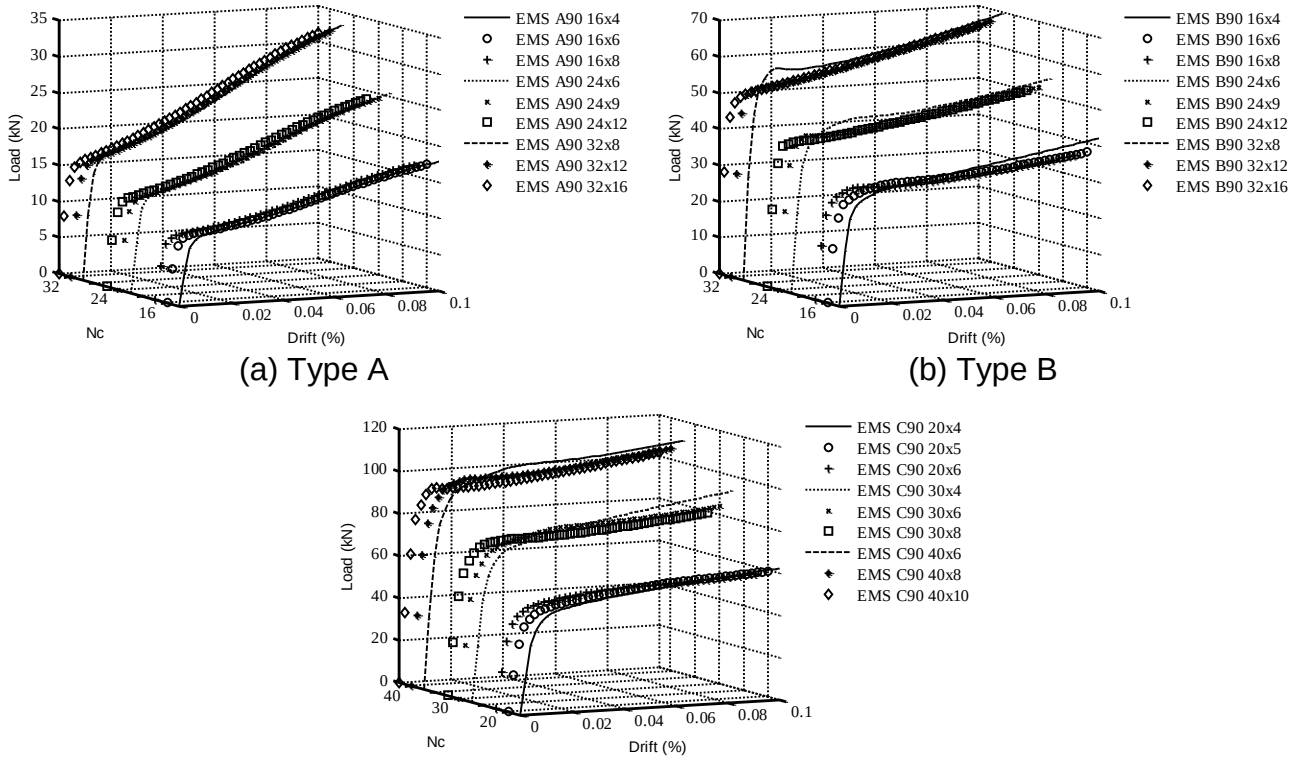

(a) Type A (b) Type B

(c) Type C

Fig. 13. Load-drift responses for EMS panels with α=90°.

Figs. 13 show the load-drift response for EMS panels oriented at 90° (EMS A90, EMS B90, and EMS C90). The global responses are similar to those observed for EMS panels oriented at 0º in Figs. 12. It is important to point out that, when comparing two EMS panels of similar sizes but with different orientations, the panels oriented at 90º have more cells in the longitudinal direction than for 0º, as seen in Table 2. Even though, the yielding loads P_y for both orientations are rather similar, as seen in Table 3, for EMS A0 8x10 $P_y = 8.64\ \mathrm{kN}$, and for EMS A90 16x4 $P_y = 8.16\ \mathrm{kN}$.

Table 3. Numerical results for EMS panels.

Panel	K_0(MN)	P_y(kN)	K_p(kN)	P_L(kN)	*Panel*	K_0(MN)	P_y(kN)	K_p(kN)	P_L(kN)
EMS A0 8x10	2.51	8.64	101.02	12.56	EMS A90 16x4	2.35	8.16	99.27	11.97
EMS A0 8x12	2.48	8.54	101.94	12.41	EMS A90 16x6	2.28	8.08	98.15	11.86
EMS A0 8x14	2.46	8.48	101.87	12.32	EMS A90 16x8	2.25	8.13	97.44	11.92
EMS A0 12x15	3.58	12.46	152.12	12.07	EMS A90 24x6	3.37	11.74	150.79	11.50
EMS A0 12x18	3.53	12.38	152.91	11.99	EMS A90 24x9	3.31	11.52	146.05	11.29
EMS A0 12x21	3.58	12.32	152.99	11.93	EMS A90 24x12	3.28	11.34	144.56	11.11
EMS A0 16x20	4.58	16.17	216.20	11.75	EMS A90 32x8	4.40	15.94	199.34	11.72
EMS A0 16x24	4.52	16.12	203.96	11.71	EMS A90 32x12	4.35	15.61	194.05	11.47
EMS A0 16x28	4.54	16.13	205.91	11.72	EMS A90 32x16	4.29	15.33	191.20	11.27
EMS B0 8x10	8.24	27.33	81.02	49.94	EMS B90 16x4	7.50	25.45	87.23	41.86
EMS B0 8x12	8.16	27.24	86.91	49.78	EMS B90 16x6	7.27	25.14	86.66	41.34
EMS B0 8x14	8.11	27.20	89.09	49.70	EMS B90 16x8	7.17	24.99	84.91	41.10
EMS B0 12x15	11.97	42.79	129.95	52.13	EMS B90 24x6	10.73	37.39	124.83	40.99
EMS B0 12x18	11.91	41.15	139.69	50.13	EMS B90 24x9	10.56	37.16	136.62	40.75
EMS B0 12x21	11.87	40.89	136.80	49.82	EMS B90 24x12	10.47	37.03	131.58	40.60
EMS B0 16x20	15.75	52.64	186.32	48.10	EMS B90 32x8	14.02	49.44	176.97	40.66
EMS B0 16x24	15.69	50.14	201.15	45.82	EMS B90 32x12	13.87	48.76	181.61	40.10
EMS B0 16x28	15.66	53.63	192.19	49.01	EMS B90 32x16	13.98	49.00	174.89	40.30
EMS C0 8x10	13.91	62.01	93.31	77.28	EMS C90 20x4	8.49	39.767	92.15	59.71
EMS C0 8x12	13.45	60.17	90.19	74.99	EMS C90 20x5	8.53	39.732	87.60	59.66
EMS C0 8x14	14.06	62.91	97.32	78.40	EMS C90 20x6	8.43	39.432	88.24	59.21
EMS C0 12x15	19.66	89.41	128.12	74.29	EMS C90 30x4	12.79	59.113	137.84	59.17
EMS C0 12x18	19.54	89.32	139.76	74.21	EMS C90 30x6	12.45	58.441	130.21	58.50
EMS C0 12x21	19.46	89.25	130.96	74.15	EMS C90 30x8	12.28	58.138	131.64	58.20
EMS C0 16x20	25.79	118.58	202.44	73.89	EMS C90 40x6	16.46	77.389	166.51	58.10
EMS C0 16x24	25.69	118.59	209.26	73.90	EMS C90 40x8	16.25	77.279	162.40	58.02
EMS C0 16x28	25.61	118.69	214.55	73.96	EMS C90 40x10	16.13	77.684	164.32	58.32

Table 5 reports the initial stiffness K_0, the yielding load P_y, the post-yielding stiffness K_p and $\mathrm{P_L}$ (the yielding load per unit panel length) of all EMS panels. First, a linear increase in panel shear strength with the number of columns can be appreciated for K_0, $\mathrm{P_y}$ and K_p parameters that also exhibit a high sensitivity toward geometry changes due to the plastic loading path.

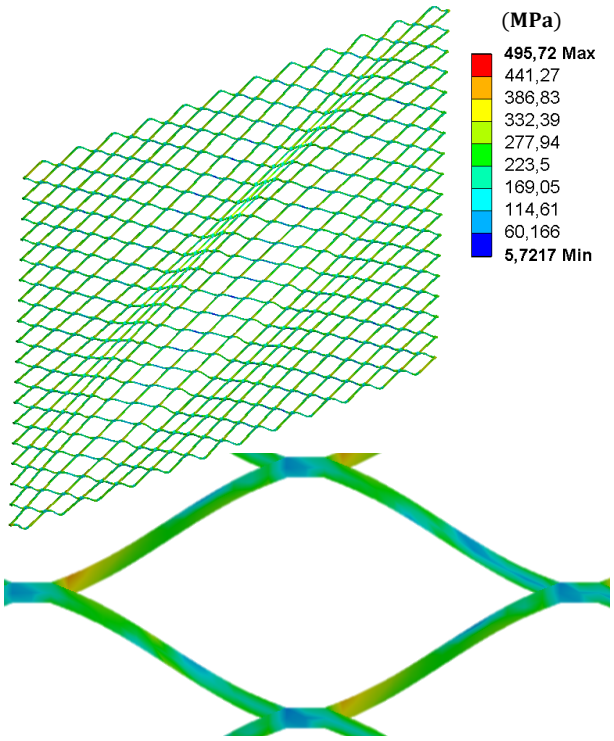

(a) EMS A0

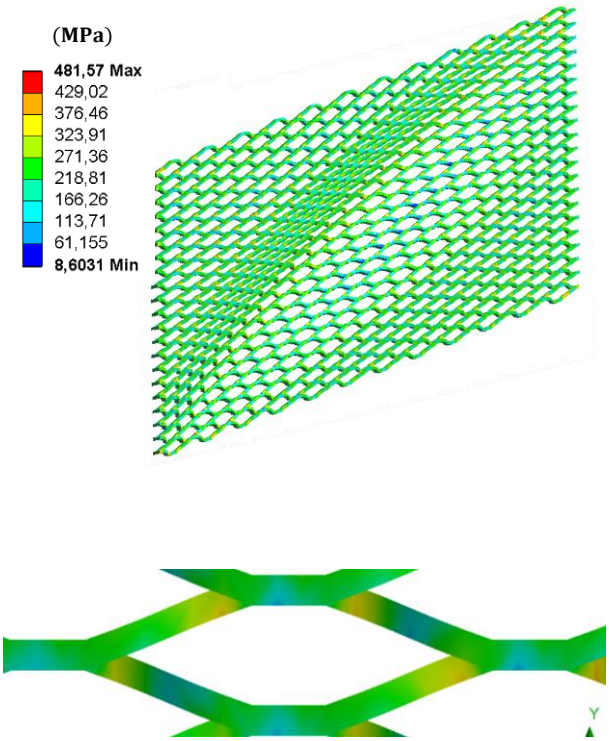

(b) EMS C0

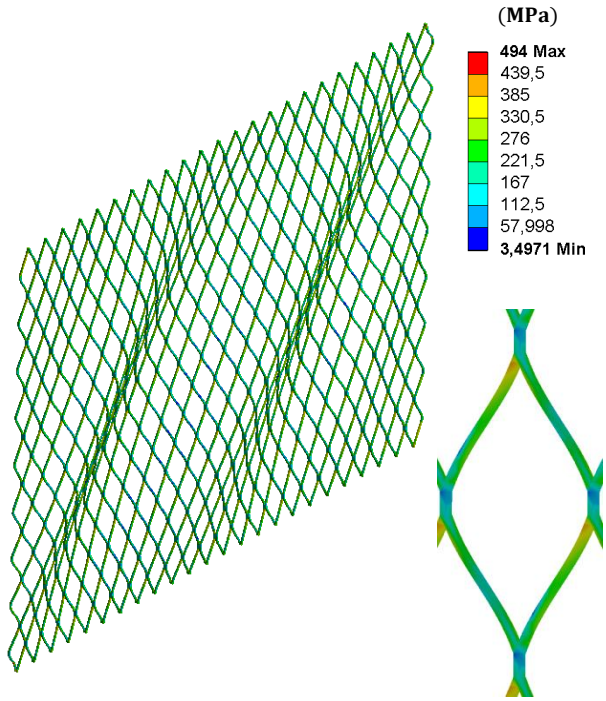

(c) EMS A90

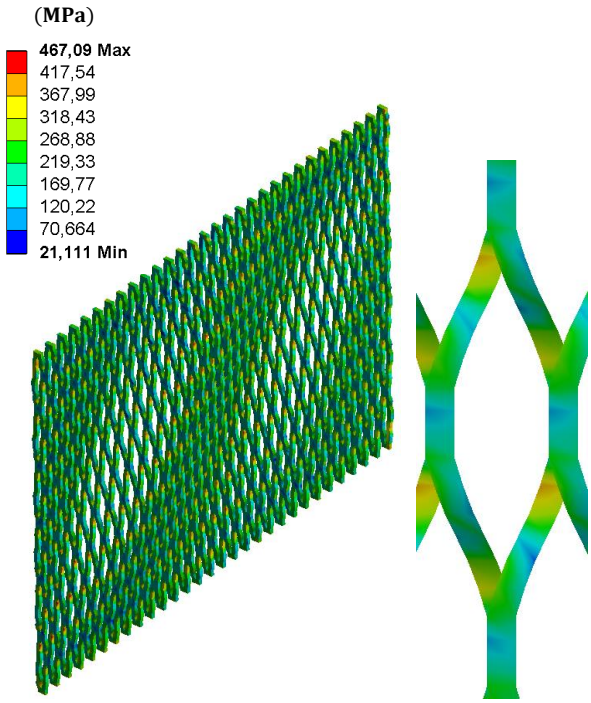

(d) EMS C 90

Fig. 14. Deformed shapes and von Mises stress distribution at failure for EMS panels.

As mentioned earlier, it is also observed that the panel height has no influence on the strength of the panel because K_0, P_y and even K_p varies less than 5% when the panel height is folded. Second, a close examination of the yielding load per unit length P_L shows that, EMS panels oriented at 0 º exhibit better performances than panels oriented at 90º for the three cell types, a result that can also be observed for the stiffness.

From the results reported in Table 3, it is possible to observe an enhancement in the loads when increasing the cell cross section. For EMS panels Type C the loads are larger than for the EMS panels Type A, for instance, the yield load for panel EMS C0 16x28 is $P_y = 118.96\,\mathrm{kN}$, and for panel EMS A0 16x28 is $P_y = 16.16\,\mathrm{kN}$, the former is 7.14 times greater than the latter.

Subsequently, each mesh type has different performance, its stiffness and yielding load is greatly dependent of cell geometry. In terms of the yield load P_y, Type B panels outperform almost four times Type A panels, meanwhile Type C panel has little improvement (1.7 times) over panel Type B. The main differences between these cells types are the aspect ratios, because meshes types A and B have a 2:1 aspect ratio, whereas type C has 4:1 aspect ratio.

Figs. 14 shows the deformed shapes and von Mises stress distributions obtained numerically for EMS panels. In all cases, it is observed that the initially straight EMS panels exhibited out-of-plane deformations at failure. For EMS panels oriented at 0°, EMS A0 (Fig. 14a) and EMS C0 (Fig. 14b), a large buckle appears along the diagonal such as a tension field action. In a like manner, for EMS panels oriented at 90°, EMS A90 (Fig. 14c) and EMS C90 (Fig. 14d), two large buckles appears. For Type C meshes the size of the buckles are minimized (Fig. 14b and 14d). In the experiments [Ref], some broken strands were observed in the diagonal corners opposite to the force application points of the testing frame.

The load-drift responses for EMS panels showed a smooth transition between the elastic and plastic regime, hence the response is rather stable. In terms of the stress

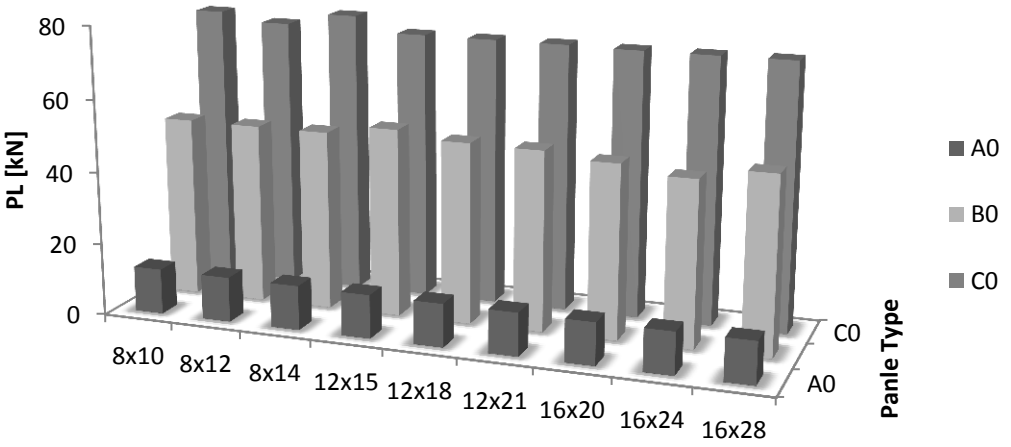

(a) Expanded metal panel EMS 0°

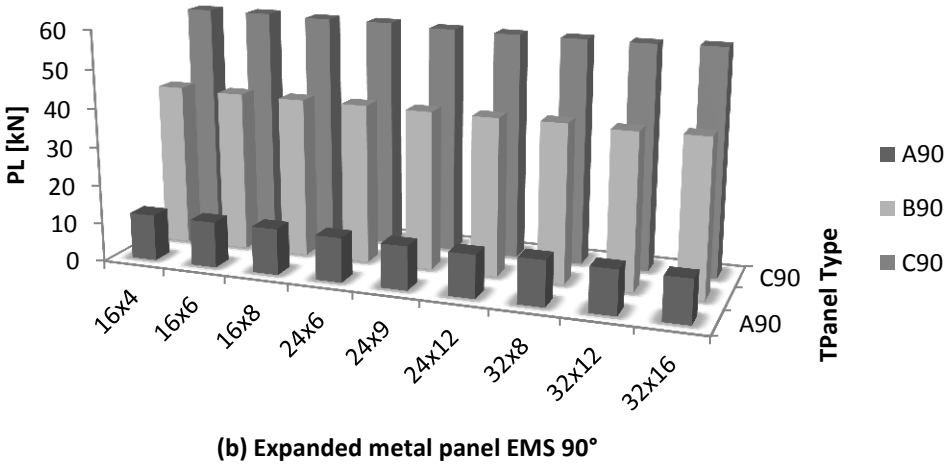

Fig. 15. Yielding load per unit panel length P_L for EMS panels.

distributions, the strands attained fully plastic deformation near their connecting nodes along the deformed diagonal as seen in Figs. 14. This plastic collapse mechanism occurs prior to global buckling. Because of the manufacturing process, EMS panels exhibit an offset between the strands, which represent initial geometric imperfections. This feature plays a very important role in the collapsibility of EMS panels; hence it is an asset for energy absorption purposes. Fig. 15 summarizes the results for the yield load per unit panel length for all the expanded metal panels investigated herein.

5. Conclusions

The structural response of expanded metal panels has been investigated herein by means of nonlinear finite element analysis that gives consistent results compared with experimental tests. From the parametric analysis, each panel is studied by calculating its initial stiffness, yielding load and post-yielding stiffness, obtaining that these parameters are greatly dependent on cell geometry, panel size and proportionally dependent on material properties.

EMS panels undergo a local deformation mechanism, which leads to cell plastic collapse and a stable load-drift response. Initial stiffness, yielding load and post-yielding stiffness only depends of the number of columns or panel length and cell geometry, hence the dependence of panel height or the number of rows could be neglected. This is an important difference when compared to solid steel plates.

Type C panels have the best performance due to its larger strand cross-section. The orientation of EM panel cells has also influence in the shear strength. Panels oriented at 0º has better performance than those oriented at 90º for the three mesh types, because the load is aligned with the main diagonal of EM cells.

Finally, cell geometry dimensions and panel length are the main parameters in order to characterize the shear response of EM panels. The stability and performance of standard panels make it suitable to investigate its application in energy absorption purposes under shear conditions.

References

Bhowmick AK. Seismic analysis and design of steel plate shear walls. PhD dissertation. Edmonton (AB, Canada): University of Alberta; 2009.

Vian D. Steel plate shear walls for seismic design and retrofit of building structures. PhD dissertation Buffalo, Buffalo, N.Y.: State Univ. of New York; 2005.

Bhowmick, A. K. (2014). Seismic behavior of steel plate shear walls with centrally placed circular perforations. Thin-Walled Structures, 75, 30-42.

Bhowmick AK, Grondin GY, Driver RG. Nonlinear seismic analysis of perforated steel plate shear walls. J Construct Steel Res 2014;94:103–13.

Egorova N, Eatherton MR, Maurya A. Experimental study of ring-shaped steel plate shear walls. J Construct Steel Res 2014;103:179–89.

Hitaka T, Matsui C. Experimental study on steel shear walls with slits. ASCE J Struct Eng 2003;129(5):586–95.

Cortes G, Liu J. Experimental evaluation of steel slit panel–frames for seismic resistance. J Constr Steel Res 2011;67(2):181–91.

Vian D, Bruneau M. Steel plate shear walls for seismic design and retrofit of building structures. Buffalo, N.Y.: State University of New York at Buffalo; 2005 (Technical report MCEER-05-0010).

Berman JW, Bruneau M. Experimental investigation of light-gauge steel plate shear walls. ASCE J Struct Eng 2005;131(2):259–67.

Expanded Metal Manufacturers Association (EMMA). Division of the National Association of Architectural Metal Manufacturers (NAAM). EMMA 557-12: standards for expanded metal; 2012.

Smith D, Graciano C, Martínez G. Recent patents on expanded metal. Recent Pat Mater Sci 2009;2(3):209–25

Graciano C, Martínez G, Smith D. Experimental investigation on the axial collapse of expanded metal tubes. Thin-Walled Struct 2009;47:953–61.

Graciano C, Martínez G, Gutiérrez A. Failure mechanism of expanded metal tubes under axial crushing. Thin-Walled Struct 2012;51:20–24.

Martínez G, Graciano C, Teixeira P. Energy absorption of axially crushed expanded metal tubes. Thin-Walled Struct 2013;71:134–46.

Smith D, Graciano C, Martínez G. Quasi-static axial compression of concentric expanded metal tubes. Thin-Walled Struct 2014;84:170–76.

Smith D, Graciano C, Martínez G. Teixeira P. Axial crushing of flattened expanded metal tubes. Thin-Walled Struct 2014;85:42–49.

Dung PN. Plumier A. Behaviour of expanded metal panel under shear loading In: Proceedings of SDSS RIO 2010 stability and ductility of steel structures 2010 p 1101–1108 [Rio de Janeiro].

Dung PN Seismically retrofitting and upgrading RC-MRF by using expanded metal panels. Doctoral thesis. University of Liege. Belgium 2011 http://hdlhandlenet/2268/100773.

ANSYS, Inc, ANSYS Release 12.0 Elements Reference, USA; 2009.

Sánchez R. Determinación de las propiedades mecánicas de láminas de metal expandido. (Master thesis) Coordinación de postgrado en ingeniería mecánica. Caracas, Venezuela: Universidad Simón Bolívar; 2005 ([In Spanish]).